Published in final edited form as:
Protein Pept Lett. 2013 May 1; 20(5): 573–583.

Functional and Structural Analysis of the Conserved EFhd2 Protein

Yancy Ferrer Acosta[1], **Eva N. Rodríguez Cruz**[1], **Ana del C. Vaquer**[1], and **Irving E. Vega**[1]
[1]Department of Biology, University of Puerto Rico-Río Piedras Campus, San Juan, PR 00931

Abstract

EFhd2 is a novel protein conserved from *C. elegans* to *H. sapiens*. This novel protein was originally identified in cells of the immune and central nervous systems. However, it is most abundant in the central nervous system, where it has been found associated with pathological forms of the microtubule-associated protein tau. The physiological or pathological roles of EFhd2 are poorly understood. In this study, a functional and structural analysis was carried to characterize the molecular requirements for EFhd2's calcium binding activity. The results showed that mutations of a conserved aspartate on either EF-hand motif disrupted the calcium binding activity, indicating that these motifs work in pair as a functional calcium binding domain. Furthermore, characterization of an identified single-nucleotide polymorphisms (SNP) that introduced a missense mutation indicates the importance of a conserved phenylalanine on EFhd2 calcium binding activity. Structural analysis revealed that EFhd2 is predominantly composed of alpha helix and random coil structures and that this novel protein is thermostable. EFhd2's thermo stability depends on its N-terminus. In the absence of the N-terminus, calcium binding restored EFhd2's thermal stability. Overall, these studies contribute to our understanding on EFhd2 functional and structural properties, and introduce it into the family of canonical EF-hand domain containing proteins.

Keywords

EFHD2; calcium binding; EF-hand domain; coil-coiled domain; tau-associated protein; secondary structure

Introduction

EFhd2 is a novel calcium binding protein conserved from invertebrates to vertebrates, suggesting that this protein may play an important physiological role that withstands the forces of evolution [1]. EFhd2 has a polyalanine motif, two EF-hand motifs and a coiled-coil domain that are highly conserved across distant taxa [1, 2]. The polyalanine motif is located at the N-terminus, while the coiled coil domain is at the C-terminus [1]. Both, polyalanine and coiled-coil, are known to promote protein-protein interactions [3]. The EF-hand motifs are known to mediate calcium binding, and these are found close to the center of EFhd2's protein sequence [1–2, 4].

EFhd2 expression is detected in most organs, but it is mainly abundant within the brain [2]. This protein was first identified in CD8 T cells, but it has also been detected in CD4 T cells

Corresponding Author: Irving E. Vega, Department of Biology, University of Puerto Rico-Río Piedras Campus, Julio García Díaz Bldg. #120, San Juan, PR 00931, Tel.: 787-764-0000 ext. 4896, irving.vega1@upr.edu.

Conflict of Interest: The authors declare that there are no conflicts of interest.

and mast cells [5–7]. In B cells, it appears to serve as a modulator of B-cell receptor (BCR) proapototic signaling [7]. Previous work showed that EFhd2 protein influences cell survival by negatively modulating the NF-kB anti-apoptotic pathway and affected calcium efflux from the endoplasmic reticulum storage [7]. In the brain, EFhd2 was found associated with the microtubule-associated protein tau in a tauopathy mouse model (JNPL3) and humans with tauopathies, such as Alzheimer's disease [2]. However, the physiological or pathological roles that EFhd2 plays in either the nervous or immune system remains poorly understood.

EF-hand domain containing proteins mediate calcium signaling pathways in the cell [3]. These calcium-binding proteins are mainly divided in two types: calcium sensors and calcium modulators. This classification is based on the structure and function of these proteins after calcium binding [8–9]. Calmodulin is the most classical example of a calcium "sensor". Calcium binding induces a conformational change in calmodulin that leads to the exposure of specific residues that enable it to associate with other proteins, such as the calmodulin-dependent protein kinase II [10]. Other calcium-binding proteins, such as calbindin D_{9K}, are classical calcium "buffers" or "modulators". Calcium binding does not induce a significant conformational change in these proteins. Members of the EF-hand calcium buffers serve as modulators of cytoplasmic calcium ions [9, 11–13]. A more recent study on EFhd2's calcium binding activity indicated that this novel protein influences the intracellular calcium concentration upon activation of the B cell receptor in WEHI231 cells [14]. However, it is still unclear if EFhd2 belongs to either of the classes of calcium binding proteins. In this study, a functional domain analysis was performed to characterize EFhd2's calcium binding activity and structural stability.

Materials and Methods

Bioinformatics Analyses

Protein Sequence alignment was made using NCBI sequences of EFhd2 for various organisms at http://www.ncbi.nlm.nih.gov/sites/entrez. EF-hand domain prediction was made using the SMART server at http://smart.embl-heidelberg.de/. Coiled-coil domain prediction was made using the COILS algorithm at: http://www.ch.embnet.org/software/COILSform.html [15]. Prediction of EFhd2 secondary structure from its primary sequence was made using the SCRATCH protein prediction tool at: http://scratch.proteomics.ics.uci.edu/index.html [16]. Protein structure prediction was carried out using the Phyre2 server (http://www.sbg.bio.ic.ac.uk/phyre2/) [17]. Mouse EFhd2 sequence was analyzed using the "Intensive Modeling Mode" on this server. The structure shown is the one obtained at a 99.9% confidence level.

Cloning of Recombinant EFhd2 Proteins

His-tagged EFhd2 proteins—The mouse EFhd2 cDNA encoding the wild type (753bps) and the C-terminus truncated mutant (594 bps) EFhd2 protein were subcloned from pIV-53 and pIV-54 respectively (constructs synthesized by IDT DNA Technologies, not shown in Table 1) to Vector pp-80L (5Prime Cat No. 2400850) between BamHI and HindIII restriction sites resulting in pIV-56 and pIV-57. Ligation reactions were transformed in *E. coli* XL-1 cells using standard procedures. Colonies were screened by colony PCR. Positive colonies were further confirmed by sequencing (Sequencing & Genotyping facility (SGf) UPR-RP and MCLAB Sequencing services).

Point mutants—His EFhd2 point mutants near and in the EF-Hand domains were generated by site directed mutagenesis (Stratagene) following manufacturer's recomendations in pIV-56 using the following primer pairs: for D105A REV 5′ GCC ATC

CCT GCC GGC GGC AGC ATA CTG CTT GAA CAT CTT CTC 3′ and FWD: 5′ GAG AAG ATG TTC AAG CAG TAT GCT GCC GCC GGC AGG GAT GGC 3′; for D141A FWD: 5′CTC AAG AGT ATG ATC CAG GAG GTG GCC GAG GAT TTC GAC AGC 3′ and REV: 5′ GCT GTC GAA ATC CTC GGC CAC CTC CTG GAT CAT ACT CTT GAG 3′; for F89L FWD 5′ CCC TAC ACC GAG TTC AAG GAG TTG TCC AGG AAG CAG ATC AAA GAC 3′ and REV 5′GTC TTT GAT CTG CTT CCT GGA CAA CTC CTT GAA CTC GGT GTA GGG 3′. All mutations were confirmed by sequencing (MCLAB sequencing services). The resulting plasmids were named pIV-60, pIV-59 and pIV-58, respectively.

The EFhd2$^{\Delta NT}$ was amplified from plasmid pIV-5 by PCR using primers FWD 5′ GCC ATA GGA TCC ATG GCC ACG GAC GAG TTG GCC 3′ and REV 5′ GCC AAT GGT ACC CTA CTT GAA CGT GGA CTG 3′. PCR were performed in a 20 μl total volume, and the reaction mixtures contained 100 ng of DNA template, 150 ng of DNA primers, 200 μM dNTPs and 0.2 μl Phusion™ DNA polymerase. PCR conditions were as follows: Initial denaturation for 4 min. at 94 °C; denaturation at 94°C for 30 seconds, annealing at 55 °C for 30 seconds, and extension at 72 °C for 45 seconds (25 cycles total). Final extension was performed at 72 °C for 7 min. PCR products were resolved in a 2% agarose gel, and 567 bps DNA fragments were isolated using Qiagen's Gel Extraction Kit (Qiagen Cat No. 28704) according to manufacturer's recommendations. DNA was then digested with BamHI and Kpn1. Plasmid pIV-35 (PerfectPro cis-repress Vector Set from 5 Prime (Cat No. 2400850) was also digested with BamHI and KpnI. PCR products were ligated into linearized plasmid. Ligation reactions were transformed in *E. coli* BL-21 cells using standard procedures. Colonies were screened by colony PCR. Positive colonies were further confirmed by sequencing (Sequencing & Genotyping facility) UPR-RP.

Recombinant Protein Purification

His tagged proteins—*E. coli* bacteria overexpressed EFhd2 His-tagged proteins full length, point mutants, N-terminus truncation and coiled-coil truncation after the addition of 0.4 mM IPTG and induction for 1 hr. Bacteria were collected by centrifugation, resuspended in a buffer composed of 150 mM sodium chloride, 50 mM Tris Base, 5 mM imidazole, pH 7.4, and lysed by sonication. The cytoplasmic fraction of the lysate was incubated with a His-tag affinity nickel column and proteins were eluted using a buffer composed of 150 mM sodium chloride, 50 mM sodium phosphate, 250 mM imidazole, pH 8. To assess purification, eluted proteins were resolved by SDS-PAGE and visualized by coomassie blue staining.

Radioactive Calcium ^{45} Binding Assays

In vitro calcium^{45} binding assay—Recombinant His-EFhd2^{WT}, His-EFhd2$^{\Delta NT}$, His-EFhd2$^{\Delta CC}$ and EF-hand motif mutants (D105A and D141A) were affinity purified from bacterial lysate using a nickel affinity column as described above. Proteins bound to the column beads were extensively washed and equilibrated with binding buffer (10 mM Tris-HCl pH 7.5, 100 mM KCl). The same amount of beads was used for each reaction and these were incubated for 30 min. with 1.3 μCi $^{45}CaCl_2$ at room temperature. After incubation, beads were washed five times with binding buffer to remove excess ^{45}Ca and added to 10 mL scintillation counter liquid. The radioactivity associated to these beads was measured using a Beckman Coulter scintillation counter (LS6500 Multi-Purpose Scintillation Counter). The amount of $^{45}CaCl_2$ bound to the beads was corrected for the amount of protein used on each reaction.

Circular Dichroism

Circular dichroism experiments were performed in an Olis™ DSM 10 CD spectrophotometer instrument, in a temperature controlled cell using a 0.2 mm quartz cuvette. Spectra of His-EFhd2^{WT}, His-EFhd2$^{\Delta NT}$, His-EFhd2$^{\Delta CC}$ and BSA secondary structure were obtained in the far-UV region (190–260 nm). All spectra were corrected against the solvent background. To study the effect of calcium binding in the secondary structure of EFhd2^{WT} and EFhd2 mutants, recombinant His-tagged proteins were purified from bacteria using a nickel affinity column. These proteins were extensively washed, eluted, dialyzed against ddH_2O and purity was assessed by SDS PAGE and coomassie staining. Protein solutions of 1.4 mg/mL for His-EFhd2 proteins (51 μM His-EFhd2^{WT}, 62 μM His-EFhd2$^{\Delta NT}$, 59μM His-EFhd2$^{\Delta CC}$) were prepared in ddH_2O to avoid absorbance of compounds in the far UV region and prevent the formation of unwanted salts when $CaCl_2$ was added. Protein quantification using UV at 280 nm was made using the extinction coefficient: 2980 $M^{-1}cm^{-1}$ for all three EFhd2 proteins. Molecular weights used for each protein were the following: His-EFhd2^{WT}: 27623.0 g/mol, His-EFhd2$^{\Delta NT}$: 22510.5 g/mol, His-EFhd2$^{\Delta CC}$: 23823.8 g/mol, as estimated by the Prot Param algorithm (http://www.expasy.ch/tools/protparam.html) [18]. Protein concentrations were also confirmed using a Bradford protein quantification assay and by SDS PAGE, resolving 1uL of purified proteins with concentration standards and staining with coomassie blue. In the BSA control experiments, purified lyophilized protein (MW 69323.4 g/mol) was resuspended in ddH_2O and 1mg/mL (14 μM) of protein was used plus or minus 1mM $CaCl_2$. For the thermal denaturation experiments, a step-wise 10°C increase was made from 25°C to 75°C, incubating 5 min. on each temperature. The spectra shown in all EFhd2 figures represent an average of 10 scans at 25°C and 75°C. These spectra were not smoothed. The secondary structural elements that composed these spectra were estimated using the CDNN software [19]. The units used to analyze the data were molar residue ellipticity (in degree cm^2 $dmol^{-1}$). The CD data was collected in milliabsorbance units (ΔA) and transformed to ellipticity θ using the relationship [$\theta = \Delta A \times 32.982$]. The molar residue ellipticity was obtained using the following relationship: [Θ] = $\theta/(10 \times n \times l \times c)$ where θ is the ellipticity (millidegrees), n is the number of amino acid residues in the protein, l is the cuvette pathlength in cm and c is the concentration in M.

A recent study has used the CDNN program to analyze a novel calcium-binding protein's far UV-CD [20]. In this program, the secondary structure total content should be as close as possible to 100 %. If this value deviates more than 10%, possibly the analyzed spectra were not correctly matched to the CDNN's protein structural database (i.e. the spectrum is very different from any other in the program database) or there is an error in the data unit conversion. The total sum is not presented on Tables 2–4. Some of the total percentages were above the 10% error threshold, mostly when analyzing spectra at 75°C (i.e. His-EFhd2$^{\Delta NT}$, 118.4%).

Statistical analyses

Student's T-test—To statistically analyze and compare the samples in the radioactive calcium binding assays was used a student's T-test, paired, with a 2 tailed distribution. Using this test was determined whether there were significant differences between two samples that came from the same two underlying populations and had the same mean. The p values returned from the T-test algorithm were considered significant if $p < 0.05$.

Results

The N- and C-terminus are not required for EFhd2 Calcium Binding Activity

The EFhd2 protein of 240 amino acids could be divided in three principal regions: N-terminus, EF-hand domain and C-terminus (Fig. 1A). The N-terminus contains a polyalanine

motif, found most frequently in nuclear proteins such as DNA-binding transcription regulators, but the specific function of this domain is still unclear [21]. EFhd2's polyalanine motif is only conserved among mammals, from mice to humans (data not shown). In contrast to the polyalanine motif, the coiled-coil domain is located at the C-terminus is highly conserved (Fig. 1A). Coiled-coils are one of the most well-characterized protein domains and they are known to mediate protein-protein interactions [4]. Conversely, calcium-binding capacity of proteins with interaction domains could be affected while associating with other proteins or ligands because of sterical constraint or induced conformation changes. In order to determine whether the N- and C-terminus of EFhd2 have an effect on its calcium binding capacity, N- and C-terminal truncation mutants were constructed and subjected to calcium binding activity assays. As previously shown, the His-EFhd2^{WT} protein binds calcium (Fig. 1B; $p < 0.002$). However, truncation of either the N- or C-terminus increased the calcium binding capacity of EFhd2 when compared to His-EFhd2^{WT} (Fig. 1B; ΔNT, $p<0.01$ and ΔCC, $p<0.001$). Radioactive calcium binding was normalized based on the amount of recombinant protein purified (Fig. 1C). Thus, the results suggest that the N- and C-terminus may affect the accessibility of calcium ions to the EF-hand motifs or the deletion promote a conformational change that enhances calcium binding.

The EF-hand Motifs are required for EFhd2 Calcium Binding

Based on sequence alignment, EFhd2 has two canonical EF-hand motifs (Fig. 2). EFhd2's predicted EF-hand motifs are found from amino acids 95–123 and 131–159. The loop in the helix-loop-helix that forms the EF-hand motif (shown as EF-loop in Fig. 2) should mediate calcium binding. The canonical EF-loops on EFhd2 are: EF-loop1, 105aa DAGRDGFIDLME 116aa, and EF-loop 2, 141aa DEDFDSKLSFRE 152aa. The other two coordinating residues are provided by a bidentate carboxylate from an acidic amino acid located in the helix closest to the C-terminus of the motif. The first residue in this loop is always an aspartate that plays an essential role in the stereochemistry of the domain's arrangement and the calcium ion positioning [3]. Mutation of this important residue has been shown to disrupt the calcium binding capacity of other EF-hand containing proteins, such as Tescalcin [22]. Additionally, mutation of the last glutamate residue (E116 and E152) on EFhd2's EF-hand loops has shown to affect its calcium binding activity [14]. Thus, in order to corroborate EFhd2's EF-hand motifs calcium-binding activity, a point mutation was made on the first aspartate residue of either EF-loop 1 (D105A) or EF-loop 2 (D141A), which are 100% conserved from human to nematodes (Fig. 2).

EFhd2 point mutants, named HIS-EFhd2^{D105A} and HIS-EFhd2^{D141A}, were generated using site-directed mutagenesis. HIS-EFhd2^{WT} was used as calcium-binding positive control, whereas nickel beads incubated with bacterial extract was used as negative control (Fig. 3A). Equal protein concentration of the purified recombinant proteins was used in the calcium-binding assay (Fig. 3B). Mutation of the first aspartate residue in either EF1 or EF2 significantly reduced the calcium binding capacity of EFhd2 (Fig. 3A). These results indicate that EFhd2 calcium binding activity depends on the integrity of both canonical EF-hand motifs.

EFHD2 gene is located within chromosome 1 in humans and chromosome 4 in mice. Interestingly, the EFHD2 gene is found in chromosome 1 at the 1p36.21 locus. On the AlzGene database, two different studies showed that the chromosome region encompassing EFHD2 gene locus has been linked to (and in a third study associated to) late-onset Alzheimer's disease [23–26]. Furthermore, chromosome 1 sequences were aligned and several single nucleotide polymorphisms (SNPs) were detected by the SNP Discovery Group, a consortium between NIH and Sanger Institute, UK (the NCBI Single Nucleotide Polymorphisms Reference Assembly at http://www.ncbi.nlm.nih.gov/SNP/index.html). Most SNPs were identified outside the coding region. However, the SNP rs12131549 was

found to introduce a missense mutation on the EFHD2 gene's coding sequence that changed a phenylalanine, at amino acid position 89, to a leucine (F89L). Previous studies using well-characterized calcium binding proteins such as Calbindin D9k and troponin C, have produced mutants with similar hydrophobic substitutions near or within the EF-hand domains to study its structural and functional consequences [8, 12, 27–28]. Thus, to evaluate whether the F89L mutation had an effect on the calcium binding activity of EFhd2, recombinant HIS-EFhd2^{F89L} was generated. Recombinant HIS-EFhd2^{F89L} mutant showed a noticeable reduction in radioactive calcium binding in comparison to HIS-EFhd2^{WT} (Fig. 3A). These results suggest that the SNP that generates the point mutation F89L could compromise the calcium binding activity of EFhd2.

Random coil and alpha helix are the predominant secondary structure in EFhd2

EFhd2 secondary structure is still unknown. All conserved domains in the EFhd2's protein sequence are known to be predominantly alpha helical [3–4, 29]. These structural units comprise most of EFhd2's protein sequence. Thus, it is very reasonable to hypothesize that EFhd2 may be a globular protein, consisting of alpha helical structures. Consistently, bioinformatics analyses using SCRATCH [16] and Phyre2 [17] protein prediction tools suggested that EFhd2 structure consisted mainly of alpha helices (Fig. 7). In order to validate the bioinformatics results, purified recombinant His-EFhd2^{WT} was subjected to circular dichroism (CD) analyses (Fig. 4). The far-UV CD spectrum (far-UV region 190–260 nm) of purified proteins gives information about the presence of several types of secondary structure, such as alpha-helix, beta-sheet, β-turn, and random coil [30–31]. The shape of the far-UV CD spectrum for proteins with large amounts of alpha helical secondary structure is quite characteristic and can be exemplified using a well-known model protein, such as Bovine serum albumin (BSA). The spectrum of BSA shows two positive peaks at 200 nm and 222 nm, and two negative peaks at 210 nm and 230 nm, characteristics of predominantly alpha helical structure (Fig. 4A). Similar profile was observed for His-EFhd2^{WT} (Fig. 4B), indicating that the secondary structure of this novel protein contains alpha helical elements.

To determine if the deletion of EFhd2's N- and C-terminus induced a structural change when compared to the native protein, CD analyses were performed. Interestingly, none of these truncations generated spectra that significantly diverged from the full length protein's secondary structure spectrum (Fig. 4C and 4D). The similarities between these mutants and the native protein spectra suggest that the absence of the N- or C-terminus fragments did not change the secondary structural organization of EFhd2, as detected by CD. Importantly, deconvolution of the CD spectra predicted that the composition of secondary structures in the EFhd2's truncation mutant proteins did not significantly deviate from those on the EFhd2^{WT} protein (Table 2).

Calcium binding can induce a conformational change as described for proteins that function as calcium sensors [10]. CD analyses were performed to determine if EFhd2 secondary structure changed upon calcium binding. Recombinant His-EFhd2^{WT} and truncation mutants were subjected to CD analysis in the presence of calcium (Fig. 4, dashed line). As control, a CD spectrum of BSA in presence of calcium was also obtained. The CD spectra obtained did not show significant deviation from that of the proteins without calcium (Fig. 4, solid line). Deconvolution of the CD spectra showed no significant change in the secondary structures between untreated and treated with calcium (Table 2). The results suggest that calcium binding does not significantly induced secondary structure changes on EFhd2 protein.

EFhd2 N-terminus and Calcium Binding Confer Thermal Stability

Calcium binding is known to confer thermal stability to some proteins [32–33]. Thus, the thermal stability of EFhd2's secondary structure was determined in the presence and absence of calcium to further characterize the effects of calcium binding upon this protein. CD analyses were performed throughout a temperature gradient from 25°C to 75°C, in presence or absence of 1 mM $CaCl_2$. The results showed that as the temperature increases to 75°C, His-EFhd2^{WT} secondary structure did not deviated from that of the native at 25°C (Fig. 5A). The presence of calcium did not change this result, suggesting that EFhd2 is a thermostable protein (Fig. 5A and 5B). As expected, the secondary structure of BSA, used as a control in these experiments, was disrupted at 75°C, regardless of the absence (Fig. 5C) or presence (Fig. 5D) of calcium. Deconvolution of the CD spectra clearly showed a significant change in BSA's secondary structure that was not observed for EFhd2^{WT} protein (Tables 3 and 4). These results indicate that EFhd2 is a thermally stable protein that can withstand temperatures of at least 75°C, regardless of its calcium biding activity.

To determine whether the C- or N-terminus influenced EFhd2's thermal stability, we performed the same experiments using the EFhd2 truncation mutants in presence or absence of 1mM $CaCl_2$ (Fig. 6). The CD analyses showed that His-EFhd2$^{\Delta NT}$ mutant is the most sensitive of all constructs when exposed to high temperatures of 75°C without calcium (Fig. 6A). Deconvolution of the CD spectra clearly demonstrated a significant deviation in secondary structure at 25°C versus 75°C (Table 3). Conversely, His-EFhd2$^{\Delta CC}$ showed not significance change in the CD spectra at 25°C versus 75°C (Fig. 6C). Thus, the presence of the N-terminus confers the thermo stability detected for the EFhd2 protein. CD analysis of His-EFhd2$^{\Delta NT}$ in presence of calcium showed no significant change in secondary structure upon temperature increase to 75°C (Fig. 6B). Interestingly, calcium binding restored the thermal stability to His-EFhd2$^{\Delta NT}$ protein. The results suggest that EFhd2's N-terminus confers structural stability, which in its absence is restored by calcium ions.

EFhd2 Structural Modeling

Deletion of either the N- or C-terminus increases the calcium binding capability of EFhd2 protein. Thus, the N- and C-terminus may preclude calcium binding activity or deletion of these domains induces a conformational change that generates a more efficient calcium binding protein. Analysis of EFhd2's protein sequence through the protein structure prediction program Phyre2 [17] modeled an extended structure at 99.9% confidence, formed predominantly of alpha helices and random coils (Fig. 7), which coincides with the CD analysis (Fig. 5). In this structure, the EF-hand motifs fold into a domain distant from the N- and C-terminus (Fig. 7, WT). Both conserved aspartate residues are located adjacent to each other (Fig. 7). The deletion of the N-terminus generates a more globular protein, maintaining the EF-hand motifs almost at the same distance as the full-length protein (Fig. 7, compare WT vs. ΔNT). The distance between the two EF-hand motifs was reduced in the C-terminus deletion mutant (Fig. 7). However, the distance between important negative charge amino acids (D105 and E116) in the same EF-hand loop did not deviate from that of the full-length protein (Fig. 7). Therefore, deletion of N- and C-terminus mutants may render the EF-hand motifs more accessible for calcium binding. In contrast, the F89L mutation induced a conformational change that reduces the distance between negative amino acids in the same EF-hand loop and between both EF-hand motifs. This conformational change may explain the HIS-EFhd2^{F89L} mutant reduced calcium binding activity. Further experiments are required to validate these structural models.

Discussion

EFhd2's EF-hand motifs are conserved from humans to nematodes, suggesting that EFhd2's calcium binding activity may be essential for its physiological role. Recently, Hagen et al. (2012) showed that EFhd2 may play a role in BCR-induced calcium flux in WEHI231 cells [14]. They tested different EF-hand loops point mutants (E116A and E152A) than the one shown here, but obtained the same results [14]. As shown here, their data also indicated that both EF-hand motifs are functional and necessary for EFhd2's calcium binding activity [14]. They concluded that one EFhd2 molecule binds two calcium ions based on equilibrium centrifugation assays [14]. Furthermore, in vivo assays using excitable ratiometric calcium indicator to monitor the BCR-induced calcium flux suggested that overexpression of EFhd2 enhances significantly the amount of free calcium detected in WEHI213 cells after stimulation with IgM antibodies [14]. Hagen et al. (2012) also showed that this phenomenon was primarily mediated by EFhd2's N-terminus domain and the first EF-hand motif [14]. Although calcium binding activity of the N-terminus deletion mutant was not measured, the results suggested that expression of N- and C-terminal deletions failed to restore the BCR-induced calcium flux in WEHI231 cells [14]. Based on our results, N-terminal and C-terminal truncations enhanced the calcium binding capability of EFhd2. Thus, it is possible that the reduced level of free calcium detected by Hagen et al. (2012) upon stimulation of WEHI213 cells could be due to the enhanced calcium binding capability of the overexpressed EFhd2 N- and C-terminus mutant. On the other hand, it is also plausible to suggest that N- and C-terminus deletion could disrupt the association of EFhd2 with other proteins required to mediate or facilitate the BCR-induced calcium flux.

EFhd2 may function as a calcium sensor involved in signal transduction pathways induced by cellular cues or insults. In cells of the immune system, EFhd2 has been associated to signaling pathways triggered by the B-cell receptor. Additionally, its expression level in B-cells modulates the apoptotic signaling pathway [5]. EFhd2 has been suggested to function as a scaffolding protein that brings together spleen tyrosine kinase, SLP-65 and PLCγ2 to mediate BCR-induced calcium flux [7]. In the central nervous system, EFhd2 has been shown to associate with the microtubule-associated protein tau [2]. The association between EFhd2 and tau was detected in the course of tau-mediated neurodegeneration [2]. In both systems where EFhd2 has been studied, calcium ions play an important signaling role. Calcium plays a crucial role in B-cell activation and fate [34]. In addition, calcium dysregulation (i.e. increased intracellular calcium levels) has been linked to the pathophysiology of neurodegenerative disorders such as Alzheimer's disease [35]. Thus, EFhd2 main physiological function and putative pathological role may be directly linked to calcium signaling pathways involved in regulating cellular fate. Further studies are required to decipher the physiological and pathological role of the novel calcium binding protein EFhd2.

Acknowledgments

The authors are grateful for the help provided by Dr. Julie Dutil in the identification of EFhd2 SNP. This work was supported by NIH-NINDS grant 1SC1NS066988 to IEV. YFA and ENRC were supported by NIH-NIGMS training grant 5R25GM061151. ACV was supported by NIH-NIGMS training grant 5T34GM007821.

Abbreviations

BCR	B-cell receptor
BSA	Bovine serum albumin
CD	Circular dichroism

Efhd2	EF-hand domain 2
GST	Glutathione-S-transferase
SNP	Single nucleotide polymorphism

References

1. Dütting S, Brachs S, Mielenz D. Fraternal twins: Swiprosin-1/EFhd2 Swiprosin-2/EFhd1 two homologous EF-hand containing calcium binding adaptor proteins with distinct functions. Cell Commun Signal. 2011; 9:2–14. [PubMed: 21244694]
2. Vega IE, Traverso EE, Ferrer-Acosta Y, Matos E, Colón M, González J, Dickson D, Hutton M, Lewis J, Yen SH. A novel calcium binding protein is associated with tau proteins in tauopathy. J Neurochem. 2008; 106:96–106. [PubMed: 18346207]
3. Nelson MR, Thulin E, Fagan PA, Forsén S, Chazin WJ. The EF-hand domain: A globally cooperative structural unit. Protein Sci. 2002; 11:198–205. [PubMed: 11790829]
4. Woolfson DN. The Design of Coiled-Coiled Structures and assemblies. Adv Prot Chem Rev. 2005; 70:79–111.
5. Avramidou A, Kroczek C, Lang C, Schuh W, Jäck HM, Mielenz D. The novel adaptor protein Swiprosin 1 enhances BCR signals and contributes to BCR-induced apoptosis. Cell Death Differ. 2007; 14:1936–1947. [PubMed: 17673920]
6. Thylur RP, Kim YD, Kwon MS, Oh HM, Kwon HK, Kim SH, Im SH, Chun JS, Park ZY, Jun CD. Swiprosin-1 is expressed in mast cells and up-regulated through the protein kinase C beta I/eta pathway. J Cell Biochem. 2009; 108:705–715. [PubMed: 19693767]
7. Kroczek C, Lang C, Brachs S, Grohman M, Dütting S, Schweizer A, Nitschke L, Feller SM, Jäck HM, Mielenz D. Swiprosin-1/Efhd2 Controls B Cell Receptor Signaling through the Assembly of the B Cell Receptor Syk and Phospholipase C gamma2 in Membrane Rafts. J Immunol. 2010; 184:3665–3676. [PubMed: 20194721]
8. Gifford JL, Walsh MP, Vogel HJ. Structures and metal-ion-binding properties of the Ca2+-binding helix-loop-helix EF-hand motifs. Biochem J. 2007; 405:199–221. [PubMed: 17590154]
9. Schwaller B. Cytosolic Ca2+ buffers. Cold Spring Harb Perspect Biol. 2010; 2:1–21.
10. Meador WE, Means AR, Quiocho FA. Modulation of calmodulin plasticity in molecular recognition on the basis of x-ray structures. Science. 1993; 262:1718–1721. [PubMed: 8259515]
11. Ababou A, Desjarlais JR. Solvation energetics and conformational change in EF-hand proteins. Protein Sci. 2001; 10:301–312. [PubMed: 11266616]
12. Skelton NJ, Kördel J, Akke M, Forsén S, Chazin WJ. Signal transduction versus buffering activity in Ca(2+)-binding proteins. Nat Struct Biol. 1994; 1:239–245. [PubMed: 7656053]
13. Wendt B, Hofmann T, Martin SR, Bayley P, Brodin P, Grundström T, Thulin E, Linse S, Forsén S. Eur J Biochem. 1988; 175:439–445. [PubMed: 3409879]
14. Hagen S, Brachs S, Kroczek C, Fürnrohr BG, Lang C, Mielenz D. The B cell receptor-induced calcium flux involves a calcium mediated positive feedback loop. Cell Calcium. 2012; 51:411–417. [PubMed: 22317918]
15. Lupas A, Van Dyke M, Stock J. Predicting coiled coils from protein sequences. Science. 1991; 252:1162–1164. [PubMed: 2031185]
16. Cheng J, Randall AZ, Sweredoski MJ, Baldi P. SCRATCH: a protein structure and structural feature prediction server. Nucleic Acids Res. 2005; 33:W72–6. [PubMed: 15980571]
17. Kelley LA, Sternberg MJ. Protein structure prediction on the Web: a case study using the Phyre server. Nat Protoc. 2009; 4:363–371. [PubMed: 19247286]
18. Gill SC, von Hippel PH. Calculation of protein extinction coefficients from amino acid sequence data. Anal Biochem. 1989; 182:319–326. [PubMed: 2610349]
19. Böhm G, Muhr R, Jaenicke R. Quantitative analysis of protein far UV circular dichroism spectra by neural networks. Protein Eng. 1992; 5:191–195. [PubMed: 1409538]

20. Bucholc M, Ciesielski A, Goch G, Anielska-Mazur A, Kulik A, Krzywińska E, Dobrowolska G. SNF1-related protein kinases 2 are negatively regulated by a plant-specific calcium sensor. J Biol Chem. 2011; 286:3429–3441. [PubMed: 21098029]
21. Albrecht A, Mundlos S. The other trinucleotide repeat: polyalanine expansion disorders. Curr Opin Genet Dev. 2005; 15:285–293. [PubMed: 15917204]
22. Gutierrez-Ford C, Levay K, Gomes AV, Perera EM, Som T, Kim YM, Benovic JL, Berkovitz GD, Slepak VZ. Characterization of tescalcin, a novel EF-hand protein with a single Ca2+-binding site: metal-binding properties, localization in tissues and cells, and effect on calcineurin. Biochemistry. 2003; 42:14553–14565. [PubMed: 14661968]
23. Bertram L, McQueen MB, Mullin K, Blacker D, Tanzi RE. Systematic meta-analyses of Alzheimer disease genetic association studies: the AlzGene database. Nat Genet. 2007; 39:17–23. [PubMed: 17192785]
24. Myers A, Wavrant De-Vrieze F, Holmans P, Hamshere M, Crook R, Compton D, Marshall H, Meyer D, Shears S, Booth J, Ramic D, Knowles H, Morris JC, Williams N, Norton N, Abraham R, Kehoe P, Williams H, Rudrasingham V, Rice F, Giles P, Tunstall N, Jones L, Lovestone S, Williams J, Owen MJ, Hardy J, Goate A. Full genome screen for Alzheimer disease: stage II analysis. Am J Med Genet. 2002; 114:235–244. [PubMed: 11857588]
25. Holmans P, Hamshere M, Hollingworth P, Rice F, Tunstall N, Jones S, Moore P, Devrieze FW, Myers A, Crook R, Compton D, Marshall H, Meyer D, Shears S, Booth J, Ramic D, Williams N, Norton N, Abraham R, Kehoe P, Williams H, Rudrasingham V, O'donovan M, Jones L, Hardy J, Goate A, Lovestone S, Owen M, Williams J. Genome screen for loci influencing age at onset rate of decline in late onset Alzheimer's disease. Am J Med Genet B Neuropsychiatr Genet. 2005; 135:24–32. [PubMed: 15729734]
26. Hiltunen M, Mannermaa A, Thompson D, Easton D, Pirskanen M, Helisalmi S, Koivisto AM, Lehtovirta M, Ryynänen M, Soininen H. Genome-wide linkage disequilibrium mapping of late-onset Alzheimer's disease in Finland. Neurology. 2001; 57:1663–1668. [PubMed: 11706108]
27. Julenius K, Thulin E, Linse S, Finn BE. Hydrophobic core substitutions in Calbindin D_{9k}: effects on stability and structure. Biochemistry. 1998; 37:8915–8925. [PubMed: 9636033]
28. Kragelund BB, Jönsson M, Bifulco G, Chazin WJ, Nilsson H, Finn BE, Linse S. Hydrophobic core substitutions in calbindin D9k: effects on Ca2+ binding and dissociation. Biochemistry. 1998; 37:8926–8937. [PubMed: 9636034]
29. Giri K, Ghosh U, Bhattacharyya NP, Basak S. Caspase 8 mediated apoptotic cell death induced by beta-sheet forming polyalanine peptides. FEBS Lett. 2003; 55:380–384. [PubMed: 14644447]
30. Kelly SM, Price NC. The use of circular dichroism in the investigation of protein structure and function. Curr Protein Pept Sci. 2000; 1:349–384. [PubMed: 12369905]
31. Kelly SM, Jess TJ, Price NC. How to study proteins by circular dichroism. Biochim, Biophys Acta. 2005; 1751:119–39. [PubMed: 16027053]
32. Kataeva IA, Uversky VN, Ljungdahl LG. Calcium and domain interactions contribute to the thermostability of domains of the multimodular cellobiohydrolase, CbhA, a subunit of the *Clostridium thermocellum* cellulosome. Biochem J. 2003; M15 372(Pt 1):151–61. [PubMed: 12570873]
33. Wijeyesakere SJ, Gafni AA, Raghavan M. Calreticulin is a thermostable protein with distinct structural responses to different divalent cation environments. J Biol Chem. 2011; 286:8771–8785. [PubMed: 21177861]
34. Scharenberg AM, Humphries LA, Rawlings DJ. Calcium signalling and cell-fate choice in B cells. Nat Rev Immunol. 2007; 7:778–789. [PubMed: 17853903]
35. Thibault O, Gant JC, Landfield PW. Expansion of the calcium hypothesis of brain aging and Alzheimer's disease: minding the store. Aging Cell. 2007; 6:307–317. [PubMed: 17465978]

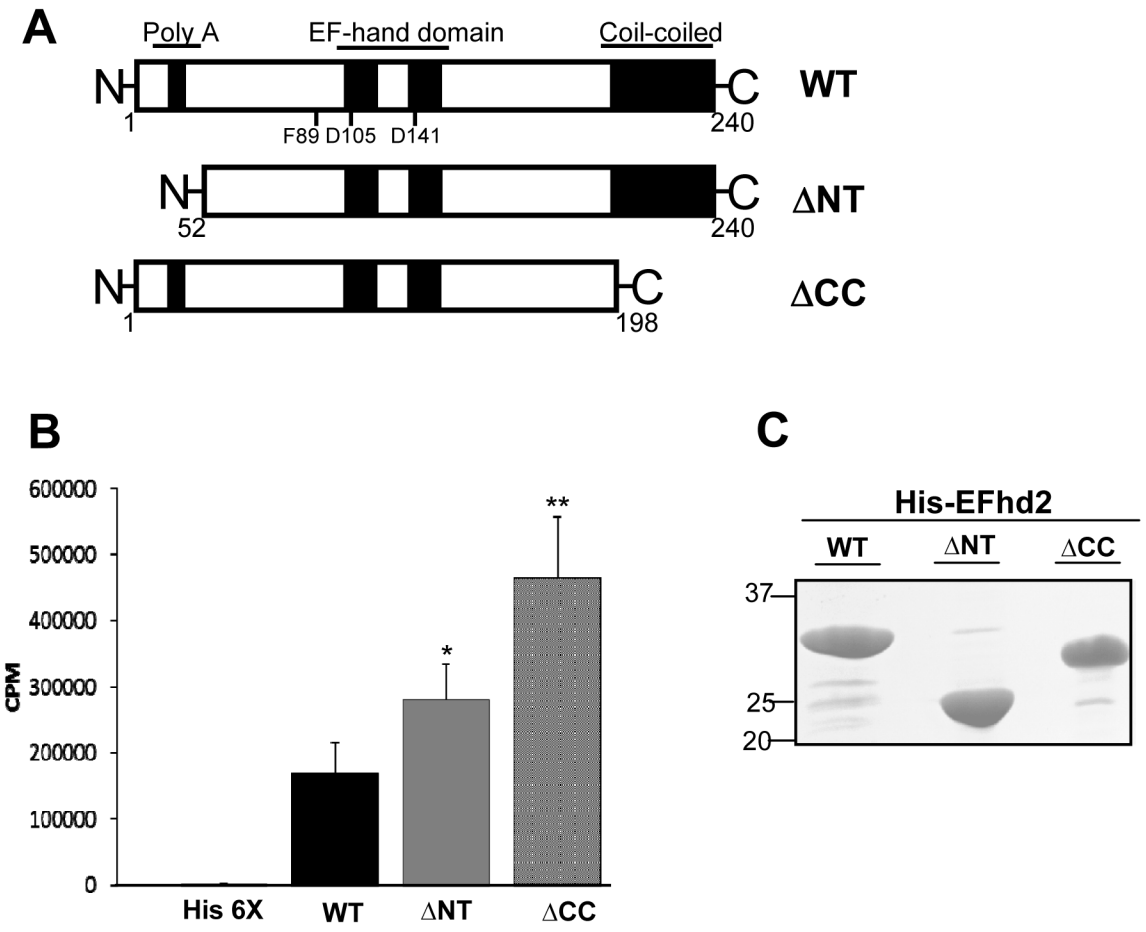

Fig. 1. His-EFhd2^{WT} and truncation mutants His-EFhd2$^{\Delta NT}$ and His-EFhd2$^{\Delta CC}$ bind calcium *in vitro*

A) Illustrated representation of EFhd2 domains under study, the N-terminus, the polyalanine domain, within the central region of the protein, the two EF-hand motifs and the coiled-coil domain at the C-terminus of the protein. The illustration is not at scale. **B)** Recombinant His-EFhd2^{WT}, His-EFhd2$^{\Delta NT}$ and His-EFhd2$^{\Delta CC}$ were purified and incubated with radioactive $^{45}CaCl_2$ to determine their calcium binding activity. Nickel-column beads were incubated with un-induced bacterial extract as negative control (His 6X). The radioactivity remaining in the beads was measured on a scintillation counter in counts per minute (*CPM*). **C)** A gel representative of the proteins used in this assay is illustrated. Protein amount was used to normalize the level of calcium binding detected. Significance was determined by a student's T-test (two-tailed, paired). Statistical significance of * $p < 0.01$ and ** $p < 0.001$ is indicated.

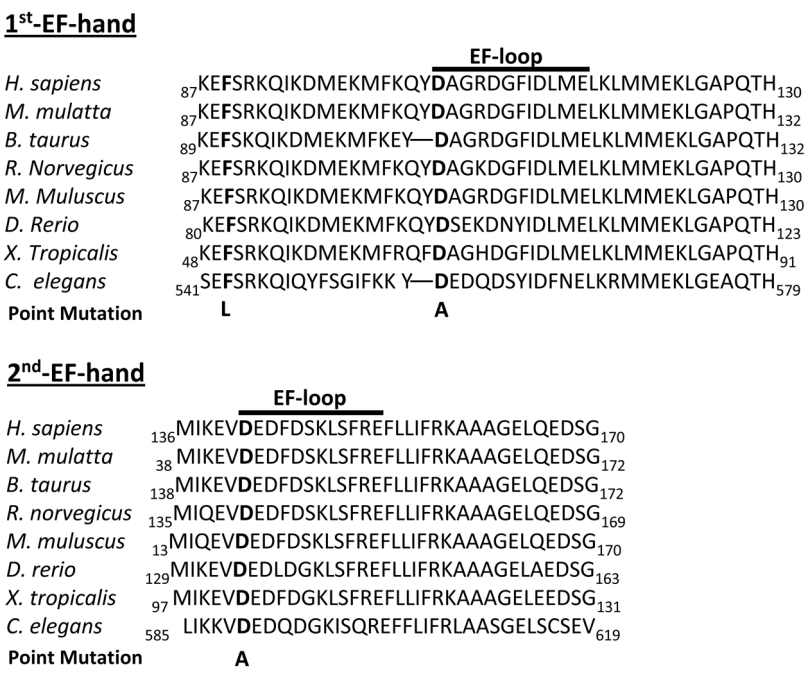

Fig. 2. EFhd2 EF-hand motifs are conserved throughout evolution

Sequence alignment of EFhd2 calcium binding motifs (1st and 2nd EF-hand motif) was performed using sequences from various species. The aspartates (***D***) in bold represent the first amino acid within each EF-hand motif loop (*EF-loop*) that is essential for the domain's calcium-binding activity. These aspartate residues were changed to alanine (***A***) by introducing a point mutation in the cDNA sequence. The phenylalanine residue (***F***) in the first EF-hand represents a conserved amino acid affected by the identified SNP rs12131549. The SNP introduces a missense mutation that changes the phenylalanine to a leucine (***L***).

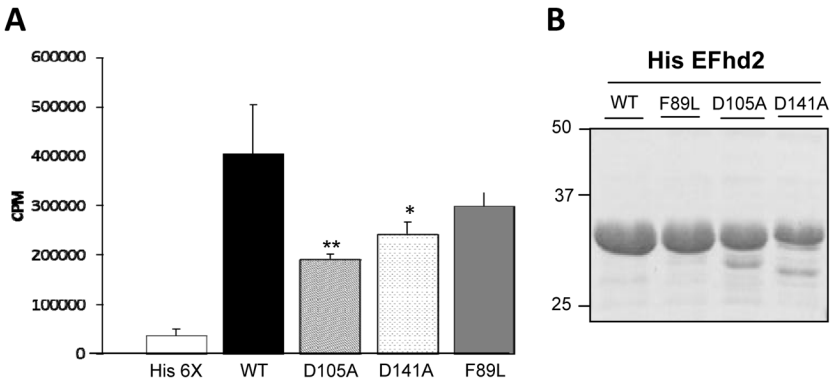

Fig. 3. Both EF-hand domains are required for EFhd2 calcium-binding affinity

A) Recombinant proteins HIS-EFhd2^{WT}, HIS-EFhd2^{F89L}, HIS-EFhd2^{D105A} and HIS-EFhd2^{D141A} were subjected to in vitro calcium binding assay using radioactive $^{45}CaCl_2$. Nickel-column beads were incubated with un-induced bacterial extract as negative control (His 6X). The amount of radioactive calcium was measured with a scintillation counter in counts per minute (*CPM*). **B)** The amount of recombinant protein was used to normalize the level of calcium binding. Significance was determined by a student's T-test (two-tailed, paired). Statistical significance of * $p< 0.02$ and ** $p<0.01$ is indicated.

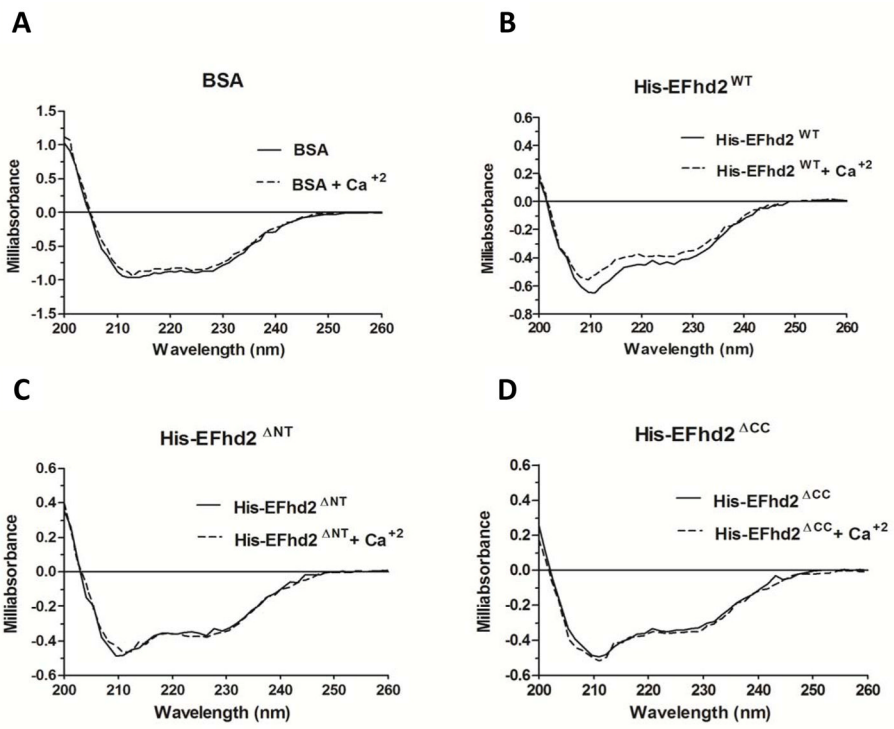

Fig. 4. His-EFhd2^{WT}, His-EFhd2$^{\Delta NT}$ and His-EFhd2$^{\Delta CC}$ secondary structure revealed by circular dichroism

A–D) Circular dichroism was used to determine changes upon calcium binding in the secondary structure of recombinant His-EFhd2^{WT} and truncation mutants at 25°C. The secondary structure of BSA (**A**), His-EFhd2^{WT} (**B**), His-EFhd2$^{\Delta NT}$ (**C**) and EFhd2$^{\Delta CC}$ (**D**) was analyzed in the far-UV region (200–260 nm) without calcium (black solid line) and with 1mM of $CaCl_2$ (dashed line). Bovine serum albumin was used as control for instrument precision and as a negative control for structural changes after addition of calcium.

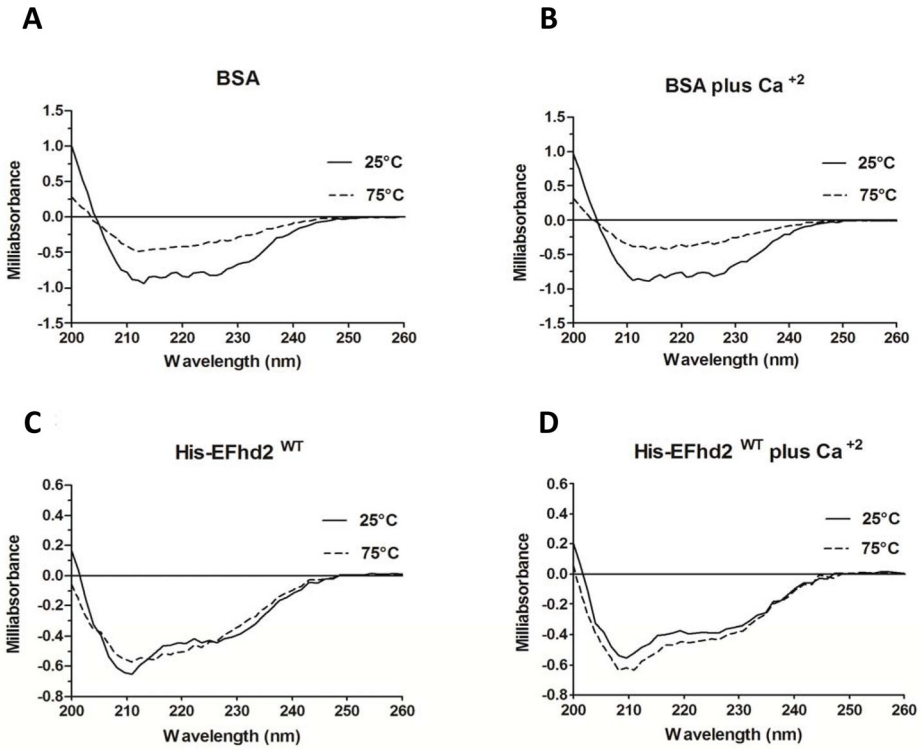

Fig. 5. Thermal stability of EFhd2^{WT}

A–**D**) Thermal stability studies on His-EFhd2^{WT} were conducted using circular dichroism. Measurements of the protein in the far-UV region (200–260 nm presented) were taken every 10°C from 25°C to 75°C. Two representative temperature spectra at 25°C (solid line) and 75°C (dashed line) are shown. The thermal stability of BSA (used as positive denaturation control) was measured in absence (**A**) or presence (**B**) of 1mM $CaCl_2$. His-EFhd2^{WT} was analyzed in the absence (**C**) or presence (**D**) of 1mM $CaCl_2$ using the same temperature range. The representative spectra at 25°C (solid line) and 75°C (dashed line) are shown.

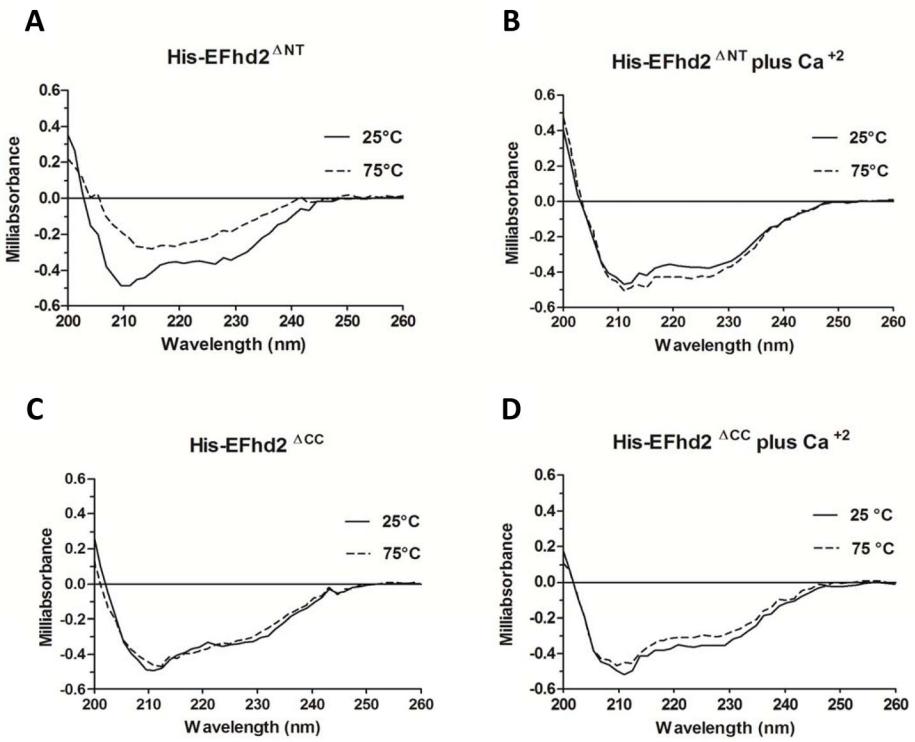

Fig. 6. The N-terminus and calcium binding are required for EFhd2's thermal stability

Recombinant His-EFhd2$^{\Delta NT}$ and His-EFhd2$^{\Delta CC}$ secondary structures were analyzed by circular dichroism to determine the contribution of the N- and C-terminus on EFhd2 thermal stability. Measurements were taken every 10°C from 25°C to 75°C in the far-UV region (200–260 nm). Two representative spectra, 25°C (solid line) and 75°C (dashed line) are shown. The effect of temperature on the structure of His-EFhd2$^{\Delta NT}$ was determined in the absence (**a**) or presence (**b**) of 1mM $CaCl_2$. The same analyses were performed for His-EFhd2$^{\Delta CC}$ without calcium (**c**) or with (**d**) 1mM $CaCl_2$. Deconvolution of the CD spectra obtained for His-EFhd2$^{\Delta NT}$ and His-EFhd2$^{\Delta CC}$ spectra are presented in Tables 3 (without calcium) and 4 (plus calcium)

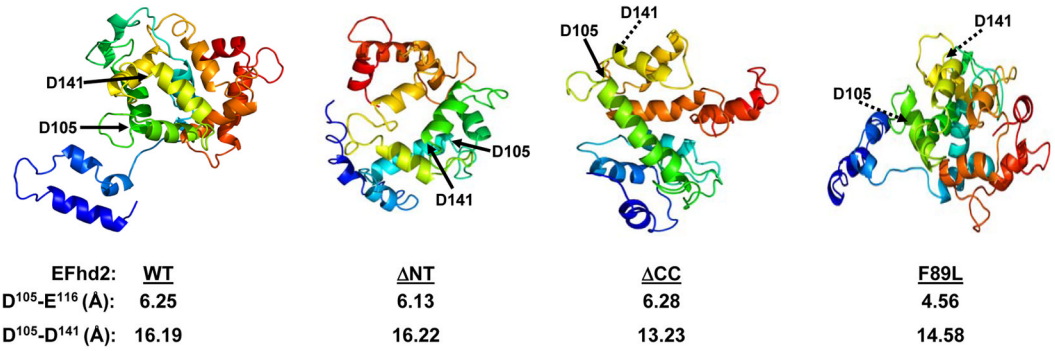

EFhd2:	WT	ΔNT	ΔCC	F89L
D^{105}-E^{116} (Å):	6.25	6.13	6.28	4.56
D^{105}-D^{141} (Å):	16.19	16.22	13.23	14.58

Fig. 7. Structural prediction of the EFhd2 protein

The mouse protein sequence of EFhd2 was analyzed using the protein structure prediction algorithms Phyre2. The predicted structures of EFhd2 wild-type (WT) protein, N- (ΔNT) and C-terminus (ΔCC) deletion mutants and EFhd2^{F89L} mutant are illustrated. The position of the conserved aspartates (D105 and D141), is indicated (arrows). Dashed arrows indicate that D105 and D141 are behind the plane. The distance (Å) between amino acids in the same EF-hand loop (D105-D116) and adjacent EF-hand motifs (D105-D141) is illustrated.

Table 1

List of constructs used to study EFhd2.

Plasmid	Plasmid name	Description	Protein name
pIV-35	pPP80	Cloning vector encompassing N-terminus 6XHistidine tag.	
pIV-38	pPP80::EFhd2$^{\Delta NT}$	EFhd2 gene sequence (567pbs) encoding for amino acids 52 to 241 cloned in to pIV-35 between BamHI and KpnI restriction sites. Encodes for His-EFhd2 ΔNT protein.	His-EFhd2$^{\Delta NT}$
pIV-56	pPP80::EFhd2	EFhd2 full length (723bps) sequence cloned into pIV-35 between BamHI and HindIII restriction sites. Encodes for His-EFhd2 full length protein.	His-EFhd2
pIV-57	pPP80::EFhd2$^{\Delta CC}$	EFhd2 gene sequence (609 bps) encoding amino acids 1 to 198 (Δ C-terminus) cloned in to pIV-35 between BamHI and HindIII restriction sites. Encodes for His-EFhd2 ΔCC protein.	His-EFhd2$^{\Delta CC}$
pIV-58	pPP80::EFhd2^{F89L}	Site directed mutagenesis of pIV-56. Point mutation from Phe to Leu at position 89.	His-EFhd2^{F89L}
pIV-59	pPP80::EFhd2^{D141A}	Site directed mutagenesis of pIV-56. Point mutation from Asp to Ala at position 141.	His-EFhd2^{D141A}
pIV-60	pPP80::EFhd2^{D105A}	Site directed mutagenesis of pIV-56. Point mutation from Asp to Ala at position 105.	His-EFhd2^{D105A}

Table 2

EFhd2 secondary structure prediction in the presence and absence of calcium.

	His EFhd2^{WT}		His EFhd2$^{\Delta NT}$		His EFhd2$^{\Delta CC}$	
Calcium	−	+	−	+	−	+
α- helix	23.8±0.6	22.7±1.2	22.2±1.3	22.4±1.7	21.5±1.2	21.7±1.1
Antiparallel β-sheet	15.7±5.4	15.9±4.5	15.5±3.7	14.7±2.7	16.8±4.9	16.9±5.1
Parallel β-sheet	11.6±0.6	12.2±1.1	12.7±1.1	12.7±1.2	12.8±1.2	12.6±1.2
β-Turn	18.8±0.3	19.1±0.3	19.0±0.4	18.9±0.5	19.3±0.3	19.3±0.3
Random coil	39.1±1.7	40.5±2.5	42.2±1.8	42.6±1.8	42.0±2.4	41.5±2.5

Table 3

Thermal stability studies and secondary structure content prediction of BSA, His-Efhd2^{WT} and His-EFhd2 mutants at 25°C and 75°C.

	BSA		His EFhd2^{WT}		His EFhd2$^{\Delta NT}$		His EFhd2$^{\Delta CC}$	
Temperature	**25°C**	**75°C**	**25°C**	**75°C**	**25°C**	**75°C**	**25°C**	**75°C**
α- helix	47.2±3.2	24.4±1.1	23.7±0.5	22.3±1.3	22.2±1.3	17.8±1.6	21.5±1.2	21.0±0.9
Antiparallel β-sheet	3.8±1.3	11.1±4.2	15.7±5.4	18.6±8.8	25.5±3.7	20.4±6.4	16.8±4.9	17.9±6.0
Parallel β-sheet	6.6±1.0	11.7±0.5	11.6±0.6	11.9±0.6	12.7±1.1	15.1±1.9	12.8±1.2	12.9±1.2
β-Turn	14.0±0.4	18.4±0.2	18.8±0.3	19.3±0.6	19.0±0.4	20.2±0.5	19.3±0.3	19.5±0.3
Random coil	29.4±4.7	40.6±1.0	39.1±1.7	39.5±1.6	42.2±1.8	47.2±2.7	42.0±2.4	42.0±2.6

Table 4

Thermal stability studies and secondary structure content prediction of BSA, His-Efhd2^{WT} and His-EFhd2 mutants at 25°C and 75°C in the presence of calcium.

	BSA		His EFhd2^{WT}		His EFhd2$^{\Delta NT}$		His EFhd2$^{\Delta CC}$	
Temperature	**25°C**	**75°C**	**25°C**	**75°C**	**25°C**	**75°C**	**25°C**	**75°C**
α- helix	46.1±3.0	23.2±0.4	22.7±1.2	23.2±0.4	22.4±1.7	23.6±1.5	21.7±1.1	20.5±1.1
Antiparallel β-sheet	4.1±1.2	14.7±4.0	15.9±4.5	14.7±4.0	14.7±2.7	13.5±2.1	16.9±5.1	18.6±6.5
Parallel β-sheet	6.8±0.9	12.3±0.7	12.2±1.1	12.3±0.7	12.7±1.2	12.2±0.9	12.6±1.2	13.1±1.3
β-Turn	14.2±0.4	18.6±0.1	19.1±0.3	18.6±0.1	18.9±0.5	18.6±0.4	19.3±0.3	19.6±0.3
Random coil	29.8±4.5	42.0±0.8	40.5±2.5	42.0±0.8	42.6±1.8	42.0±1.1	41.5±2.5	42.2±2.9